Journal of Electrochemical Science and Technology
Vol. 3, No. 2, 2012, 57-62
http://dx.doi.org/10.5229/JECST.2012.3.2.57

THE KOREAN ELECTROCHEMICAL SOCIETY **Journal of Electrochemical Science and Technology**

Electrochemical Synthesis of Dumbbell-like Au-Ni-Au Nanorods and Their Surface Plasmon Resonance

Yeon Ju Park[a,b], Lichun Liu[a,b], Sang-Hoon Yoo[a,b], and Sungho Park[a,b,†]

[a]*Department of Chemistry, SungKyunKwan University, Suwon, Gyeonggi-Do 440-746, Korea*
[b]*Department of Energy Science, SungKyunKwan University, Suwon, Gyeonggi-Do 440-746, Korea*

ABSTRACT :

In this report, we demonstrate that the longitudinal localized surface plasmon resonance mode can be suppressed when the nanorods were in dumbbell shape. The seed nanorods were synthesized by electrochemical deposition of metals into the pores of anodic aluminum oxide templates. The dumbbell-like nanorods were grown from seed Au-Ni-Au nanorods by a rate-controlled seed-mediated growth strategy. The selective deposition of Au atoms onto Au blocks of Au-Ni-Au nanorods produced larger diameter of Au nanorods with bumpy surface resulting in dumbbell-like nanorods. The morphology of nanorods depended on the reduction rate of $AuCl_4^-$, slow rate producing smooth surface of Au nanorods, but high reduction rate producing bumpy surface morphology. Through systematic investigation into the UV-Vis-NIR spectroscopy, we found that the multiple localized surface plasmon resonance (LSPR) modes were available from single-component Au nanorods. And, their LSPR modes of Au NRs with bumpy surface, compared to the smooth seed Au NRs, were red-shifted, which was obviously attributed to the increased electron oscillation pathways. While the longitudinal LSPR modes of smoothly grown Au NRs were blue-shifted except for a dipole transverse LSPR mode, which can be interpreted by decreased aspect ratio. In addition, dumbbell-like nanorods showed an almost disappeared longitudinal LSPR mode. It reflects that the plasmonic properties can be engineered using complex nanorods structure.

Keywords : Electrochemical deposition, Nanorod, Surface Plasmon, Dumbbell, AAO

Received April 12, 2012 : Accepted June 20, 2012

1. Introduction

Collective excitations of the conduction electrons on metal surface can be induced by electro-magnetic irradiation. This phenomenon is known as surface plasmon resonance (SPR) on planar surfaces or localized surface plasmon resonance (LSPR) on nanometer scale metallic nanostructure.[1-3] LSPR of metal nanostructures have been found applications in many fields, such as photonics, electronics, optic device and catalysis.[4] By previous studies in the field, it has been known that the LSPR spectral features of metal nanostructures can be sensitively tuned by size, geometry, composition of nanostructures and surrounding medium.[5-7] In recent years, the influence of the geometry of metal nanostructures on the surface plasmon resonance has been intensively investigated. For instance, two types of plasmon resonances can appear on nanorods (NRs), which are associated with surface electrons oscillation along the short axes (transverse mode) and long axes (longitudinal modes).[8] Especially, Au NRs have distinct optical properties due to their strong optical activity and tunable UV-Vis-NIR dipole plasmon resonances on shapes and dimensions.[9,10] That is the reason why Au is commonly used as study object in plasmonics. To the best of our knowledge, the optical study on dumbbell-like Au

†Corresponding author. Tel.: +82-31-299-4562
E-mail address: spark72@skku.edu

nanorods is still in blank. In this work, we used convenient electrochemical deposition method to produce seed nanorods, including single-component Au nanorods and three-block Au-Ni-Au nanorods. By a solution-phase growth method, we successfully synthesized dumbbell-like Au-Ni-Au nanorods. The plasmonic behavior of each type of nanorods was systematically investigated. The suppressed longitudinal LSPR mode on dumbbell-like Au-Ni-Au nanorods is a new direction on engineering plasmonic output of nanostructures.

2. Experimental Section

2.1. Synthesis of AAO membrane templates

The synthetic procedure is based on the method established by Masuda et al.[11] A high-purity (99.999 %) thin plate of aluminum (from Goodfellow Cambridge Limited) was electro-polished in a mixture of ethanol (from Samchun Chemical) and perchloric acid (from Samchun Chemical) (7:3, v/v) at 20 V and 0°C for 3 min. Then the plate was anodized in 0.3 M oxalic acid (from Sigma-Aldrich) at 40 V and 0°C for 12 hours. The alumina layer was then dissolved using an aqueous mixture of chromic acid (from Sigma-Aldrich) (1.8 wt %) and phosphoric acid (from Samchun Chemical) (6 wt %), at 60°C for 12 hours. A second anodization step was conducted in 0.3 M oxalic acid at 40 V and 0°C for 24 hours, producing highly ordered porous anodized aluminum oxide (AAO) template. The residue of aluminum plate was next removed by immersing in a saturated $HgCl_2$ aqueous solution for 6 hours and then immersed in 8.5 wt % phosphoric acid solution for pore widening for 30 min. The resulting pore diameter was 85 (±5) nm.

2.2. Seed nanorods synthesis

A thin layer of Ag (~300 nm) was thermally evaporated onto one side of a nanoporous AAO template, which served as the working electrode in a three-electrode electrochemical cell after making physical contact with a aluminum foil in Teflon cell. A Pt wire and Ag/AgCl electrode were used as the counter and reference electrode, respectively. The interior of the nanopores was filled with Ag (ACR silver RTU solution from Technic Inc.) at a constant potential, –0.95 V, by passing 0.5 C/cm^2. In order to get smooth single-component Au NRs, Au atoms were then electrochemically deposited into the empty space of AAO channels at –0.95 V by using commercial plating solution of Au (from Technic Inc.). Depending on the transported total amount of charges, the length of nanorods could be flexibly controlled. Typically, 0.09 C deposition results in 100 nm of smooth NRs when the exposed apparent surface area is ~0.9 cm^2. For Au-Ni-Au three-block NRs, they were sequentially electroplated from Orotemp 24 RTU plating solution (from Technic Inc.) and nickel sulfamate RTU solution (from Technic Inc.) at –0.95 V (Scheme 1). Each block length was also under control by monitoring the charge passed through the cell. After electrochemical filling of target metal block into nanopores of AAO template, Ag conducting layer and AAO were etched out with concentrated nitric acid for 5 minutes and 3 M sodium hydroxide solutions for 30 minutes, sequentially. The resulting NRs were then rinsed with deionized water for 5 times and finally dispersed into D_2O in Ependorf tubes for use as seed NRs.

2.3. Seed-mediated synthesis

1 mL seed Au NRs solution containing 0.05 M cetyltrimethylammonium bromide (CTAB, from Fluka) was firstly mixed using a shaker machine (Combi-sv120, FinePCR) for 1 hour (defined as solution s1). Growth solution (~10 mL) contained in a 30 mL glass bottle comprised of 0.5 mM $HAuCl_4 \cdot 3H_2O$, 0.05 M CTAB, 5 μM NaOH, 5 μM ascorbic acid (defined as growth solution, g1). In another high concentration of growth solution (~10 mL), 12.5 μM instead of 5 μM ascorbic acid (AA, from Kanto) was

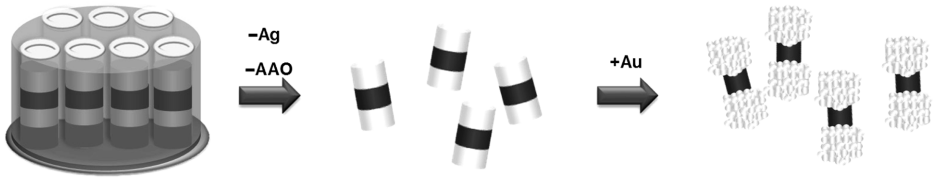

Scheme 1. The synthetic procedure of dumbbell-like Au-Ni-Au nanorods. Au-Ni-Au three-block nanorods were fabricated by the aid of anodic aluminum oxide template and electrochemical deposition. After releasing three-block nanorods, Au atoms were further selectively grown on Au surface of three-block nanorods by using solution-phase chemical growth.

used (defined as growth solution, g2). Adding s1 into gl, and following 6 hours mixing, the smoothly grown NRs were obtained. In contrast, adding s1 into g2 could produce NRs with bumpy surface. Resulting NRs were collected by centrifugation and rinsed by deionized water. The dumbbell-like Au-Ni-Au NRs were synthesized using three-block seed NRs and similar recipe as described above.

2.4. Determination of diameter and length of nanorods

The diameter and length data used in this paper were collected by averaging the values of more than 50 nanorods.

3. Result and Discussion

3.1. Synthesis and plasmonic characteristics of single-component Au NRs

Fig. 1(A) shows a typical field-emission scanning electron microscopy (FESEM) image of single-component 1D Au NRs that functioned as seeds for further formation of lager Au NRs with different surface morphologies. The morphological changes were realized by varying growth solution conditions. Firstly, we used the seed Au NRs with length ~320 nm to observe the LSPR features in the optical window of UV-Vis-NIR region. The dipole transverse mode of seed NRs appeared at 538 nm and the higher-order (quadrupole), longitudinal mode at 733 and 1444 nm (spectrum a in Fig. 1(D)), respectively. Then, we studied the change of plasmonic features after growing Au atoms onto the surface of seed NRs with a low and a high reduction rate. Fig.1(B) and 1(C) show, respectively, FESEM images of Au NRs fabricated by the seed-mediated growth strategy. Au ions in growth solution were reduced to atoms by ascorbic acid onto the surface of seed NRs.[12] This chemical reaction may be dynamically controlled by the concentration of reducing agent. By controlling the rate of chemical reaction, we obtained Au NRs with different morphologies. Therefore, the surface morphology of Au NRs may be controllable by varying the growth conditions. In a low concentration of AA and NaOH (0.1 M) in growth solution, the reduction rate of Au cations was much slowed, inducing ordered arrangement of reduced Au atoms. It was evidenced from the smooth surface of resulting NRs and increased diameter. The diameter and length of grown NRs were observed to be ~90 nm and ~335 nm, respectively. The corresponding aspect ratio of grown Au NRs was decreased from 4.00 for seed NRs to 3.72 for grown NRs (Fig. 1(B)). The dimensional change of as-grown NRs led to a red-shift of transverse LSPR mode and a blue-shift of both higher order and longitudinal LSPR modes (spectrum b in Fig. 1(D)). In an elevated concentration of AA (0.25 M) and NaOH (0.2 M) in growth solution, the reduction rate of Au ions was quickened. As a result, bumpy surface (Fig. 1(C)) of grown NRs was generated due mainly to the rapid and irregular arrangement of quickly generated Au atoms. The diameter and length of bumpy Au NRs also increased, up to ~110 nm and ~370 nm, respectively. The aspect ratios of these bumpy NRs were down to 3.36. The diameter of formed islands on the surface of Au NRs was up to ~23 nm. The LSPR modes usually shift as a function of aspect ratios. The larger aspect ratio can cause obvious red-shift of both transverse and longitudinal LSPR modes. However, all LSPR modes on these bumpy NRs shifted to longer wavelength compared to those of seed smooth NRs, as revealed in spectrum c in Fig. 1(D). This phenomenon actually accounts for the real elec-

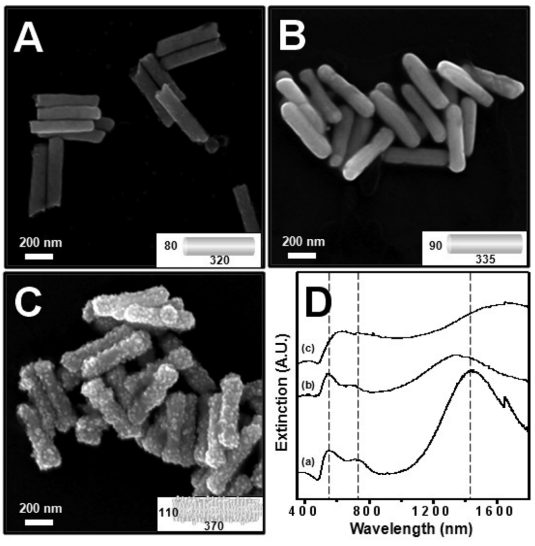

Fig.1. FESEM images of (A) pure Au NRs (L = 320 nm and d = 80 nm), (B) grown Au NRs (L = 335 nm and d = 90 nm), and (C) bumpy NRs (L = 370 nm and d = 110 nm). NRs shown in panel B and C were obtained from seed-mediated chemical growth. (D) UV-Vis-NIR extinction spectra for samples A, B and C corresponding to (a), (b) and (c), respectively. All samples were in D_2O environment. All spectra are normalized to the wavelength at 200 nm.

tron oscillation pathway distance. Even apparent aspect ratio decreased, the real aspect ratios, in actual, increased because of bumpy surface of NRs, which increased the electrons oscillation length between both ends of NRs.

And, another difference between spectra is on band width. The band of bumpy NRs was broadened compared to that of grown smooth NRs and seed smooth NRs. The surface roughness attributed to the band broadening, which was probably induced by inconsistent oscillation pathways of surface electrons. The longer distance of electrons oscillation contributed the peak at longer wavelength, and short distance of electrons oscillation contributed the peak at shorter wavelength. The overlapping of peaks at a range of wavelengths accordingly produced the wide peak. Through controlling the surface morphology of Au NRs, we investigated the change of LSPR behaviors on different NRs. When the aspect ratios of Au NRs were beyond ~4, the phase retardation of applied field inside the material caused the multi-pole resonance (higher-order harmonics).[13] Fig. 2(A) shows the FESEM image of seed Au NRs with length ~445 nm (aspect ratio, 5.36), which were used to observe the quadrupole mode. Choosing this length was according to our accumulated experience on the topic. Obvious higher-order mode (quadrupole) appeared at

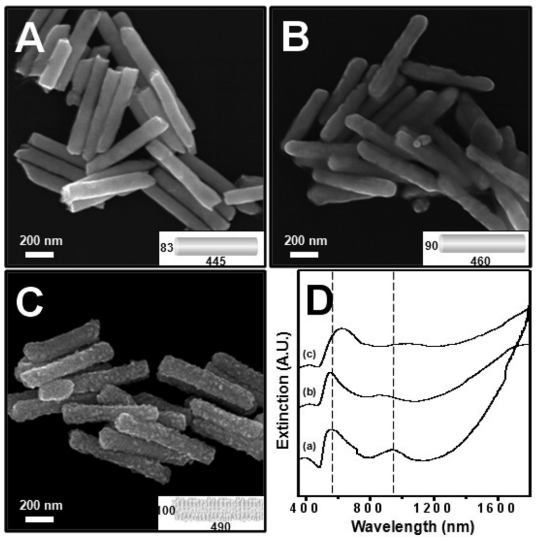

Fig. 2. FESEM images of the longer length of NRs as used in Fig. 1. The average total lengths and diameters were (A) 445 nm and 83 nm, (B) 460 nm and 90 nm, (C) 490 nm and 100 nm.

935 nm and the whole dipole LSPR mode was invisible below the wavelength of 1600 nm just leaving a peak tail around 1600 nm (Fig. 2(D), spectrum a). When the seed NRs were grown to typical larger smooth ones, the diameter and length increased to 90 nm and 460 nm, respectively (Fig. 2(B)). Though, the diameters of grown NRs increased, the quadrupole and longitudinal modes shifted to blue principally because of the less increased lengths (inducing decreased aspect ratios from 5.36-5.11). When the bumpy NRs (Fig. 2(C)) were formed via adjusting reaction conditions, we could observe longitudinal LSPR mode at 1600 nm (spectrum c, Fig. 2(D)) unlike those of seed (spectrum a) and grown smooth NRs (spectrum b). This distinct feature resulted from the damping effect and geometry factors[14,15] due to the deep roughness. Herein, aspect ratio could not be simply useful in evaluating plasmonic behavior change upon the aspect ratios. The surface roughness dominated the plasmonic properties, in this case.

3.2. Dumbbell-like Au-Ni-Au NRs and their optical responses

The three-block NRs, rather than one block, were further used to investigate how plasmonic behavior change depends on the surface states. Fig. 3(A) gives a typical SEM image of 1D three-block Au-Ni-Au nanostructure, which shows a narrow size distribution. The original Au-Ni-Au NRs were 445 nm of total length (155:135:155 nm). This shorter Ni block than an Au block cannot inhibit the plasmonic coupling between two Au blocks.[14] As a result, the transverse and quadrupole modes clearly appeared as indicated by spectrum a in Fig. 3(E). It has already been reported that optically inactive short Ni block can allow the occurrence of plasmonic coupling.[14] Using three-block Au-Ni-Au NRs as seeds, we found that the Au atoms could be selectively grown on Au parts, without detectable influence on Ni part, causing larger diameter of Au blocks than Ni ones. Therefore, dumbbell-like NRs were formed as shown in Fig. 3(B). Even though, we have controlled the concentration of reducing agent, the smooth surface of Au segments was not achieved (Fig. 3(B)). The grown Au atoms made the surface of Au blocks rough, however, Ni parts maintained smooth and unaffected. The crystal lattice mismatch between Au and Ni should be responsible for this selectivity, we think. The diameter and roughness of Au parts in Au-Ni-Au NRs varied as a

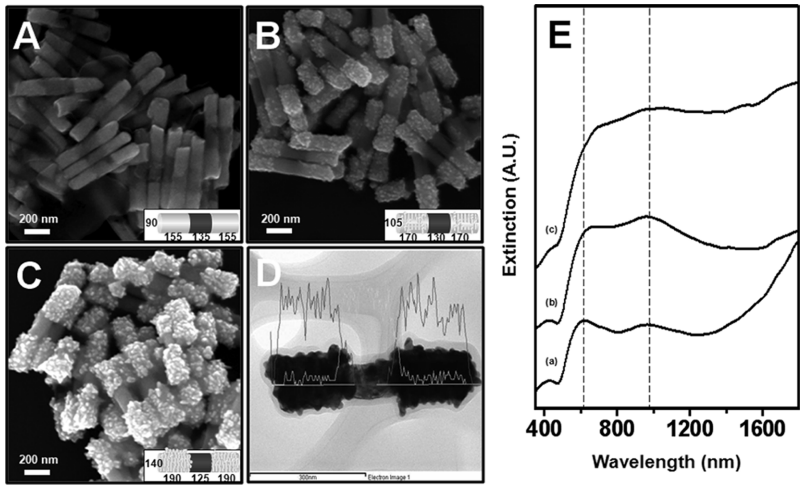

Fig. 3. FESEM images of (A) multi-block Au-Ni-Au NRs (L = 445 nm and d = 90 nm), (B) dumbbell-like Au-Ni-Au NRs (L = 470 nm and d = 105 nm), and (C), dumbbell-like Au-Ni-Au NRs (L = 505 nm and d = 140 nm). (D) An EDS line profile of sample c, red trace indicating Au atoms distribution. (E) UV-Vis-NIR extinction spectra (a), (b) and (c) corresponding to samples A, B and C. All extinction spectra of samples were measured in D_2O. All spectra have been normalized to a wavelength at 200 nm.

function of the Au ions concentration used in growth solution. When 5 μM ascorbic acid existed in growth solution, the diameter of Au blocks in three-block NRs was ~90 nm (Fig. 3(B)), when 12.5 μM ascorbic acid, the diameter increased to ~100 nm (Fig. 3(C)). The diameter difference between grown Au block and unaffected Ni block was highlighted using high resolution TEM image and their elemental mapping (Fig. 3(D)). Fig. 3(D) represents the extinction spectrum of each sample in Fig. 3(A)-(C). Spectrum a in Fig. 3(E) corresponds to seed Au-Ni-Au NRs, which were synthesized by sequential electrochemical deposition into AAO nanopores, as seen in Fig. 3(A). The transverse mode at 610 nm, quadrupole mode at 964 nm, and a longitudinal mode above 1600 nm were successfully observed. The appearance of quadrupole mode could prove the happening of plasmonic coupling between two Au blocks at the ends. For a little increased diameter of dumbbell-like NRs in Fig. 3(B), the transverse mode and quadrupole mode still occurred as shown in Fig. 3(E)(b). But, longitudinal mode was significantly suppressed. When the diameter of Au blocks further increased to ~100 nm, the peak broadening made spectrum c (in Fig. 3(E)) showing less features. To notice, the longitudinal mode quite resembles that in Fig. 3(E)(b). This suppression of longitudinal mode was due to diameter difference between Au and Ni blocks. Until now, the more solid evidences are needed to clarify the exact mechanism how diameters affect plasmonic resonance on dumbbell-like Au-Ni-Au NRs.

4. Conclusion

In conclusion, we used electrochemical deposition technique in combination with anodic aluminum oxide template to synthesize seed nanorods, from which, we further synthesized dumbbell-like nanorods by solution-phase chemical growth. The optical properties of seed Au nanorods, smoothly grown Au nanorods, bumpy Au nanorods, and dumbbell-like Au-Ni-Au nanorods were systematically investigated. The morphologies of nanorods affect plasmonic properties significantly. In particular, the diameter differences between Au and Ni blocks in dumbbell-like nanorods play an important role in suppressing longitudinal surface plasmon mode. This new finding will be useful in engineering plasmonic outcome of rod-like and/or dumbbell-like nanostructures.

Acknowledgment

This work was supported by the National Research Foundation of Korea (National Leading Research Lab: 2011-0027911).

References

1. M. E. Stewart, C. R. Anderton, L. B. Thompson, J. Maria, S. K. Gray, J. A. Rogers and R. G. Nuzzo, *Chem. Rev.*, **108**, 494 (2008).
2. W. L. Barnes, A. Dereux and T. W. Ebbesen, *Nature*, **424**, 824 (2003).
3. H. M. Bok, K. L. Shuford, S. Kim, S. K. Kim and S. Park, *Nano Lett.*, **8**, 2265 (2008).
4. S. Kim, S. K. Kim and S. Park, *J. Am. Chem. Soc.*, **131**, 8380 (2009).
5. S. Sheikholeslami, Y. W. Jun, P. K. Jain and A. P. Alivisatos, *Nano Lett.*, **10**, 2655 (2010).
6. Z. Jiao, H. Xia and X. Tao, *J. Phys. Chem. C*, **115**, 7887 (2011).
7. C. *J.* Noguez, *Phys. Chem. C*, **111**, 3806 (2007).
8. P. K. Jain, S. Eustis and M. A. El-Sayed, *J. Phys. Chem. B*, **110**, 18243 (2006).
9. B. N. Khlebtsov and N. G. Khlebtsov, *J. Phys. Chem. C*, **111**, 11516 (2007).
10. M. Grzelczak, J. Pérez-Juste, F. J. García de Abajo and L. M. Liz-Marzán, *J. Phys. Chem. C*, **111**, 6183 (2007).
11. H. Masuda and K. Fukuda, *Science*, **268**, 1466 (1995).
12. N. R. Jana, L. Gearheart and C. J. Murphy, *Chem. Mater.*, **13**, 2313 (2001).
13. E. K. Payne, K. L. Shuford, S. Park, G. C. Schatz and C. A. Mirkin, *J. Phys. Chem. B*, **110**, 2150 (2006).
14. S. Kim, K. L. Shuford, H.-M. Bok, S. K. Kim and S. Park, *Nano Lett.*, **8**, 800 (2008).
15. H. M. Bok, K. L. Shuford, E. Jeong and S. Park, *Chem. Comm.*, **46**, 982 (2010).